

**EXPERIMENTAL AND NUMERICAL STUDY OF THE FREE SURFACE ELEVATION OVER
THE PONTOONS OF A SEMISUBMERSIBLE PLATFORM IN WAVES**

João Pessoa
Wood
Sandefjord, Norway

Carl Trygve Stansberg
Ctstansberg Marinteknikk
Trondheim, Norway

Nuno Fonseca
SINTEF Ocean
Trondheim, Norway

Manuel Laranjinha
Wood
Sandefjord, Norway

ABSTRACT

The region over the pontoons, especially in the vicinity of columns, is typically a critical area in terms of upwell when analyzing the air gap of semisubmersible platforms. There is indication that numerical computations using potential flow theory may in some cases overestimate the free surface elevation in this region. To assess the possibility, experimental data is compared to numerical computations in three locations under the deck box: one location over the pontoons, one location in the vicinity of the pontoons and one location between the pontoons. The data was acquired in FORCE's towing tank facility, in Lyngby, Denmark, by relative wave gauges fixed to the moored semisubmersible platform. The experimental data is treated in order to remove the global motions from the upwell signal. The resulting free surface elevation, which includes contributions from incident, diffracted and radiated wave fields, is compared to the disturbed free surface elevation calculated with linear diffraction-radiation theory.

The study is initially conducted in irregular waves, where simulation statistics in 4 different sea states are compared to the experiments and the observed nonlinear effects are discussed. The extreme crest heights are compared with non-Gaussian models as defined in DNVGL-OTG-13 and as defined by Stansberg (2014). The study is then extended to regular waves. In a first stage we estimate the first harmonic components by removing all higher order effects, and compare the results to linear theory. For these band-pass filtered signals it is shown that results calculated with linear theory tend to overestimate free surface elevation in the location over the pontoons, but seem to correlate well with the experiments in the other locations. In a second stage the experimental crest heights are

compared with non-linear models as defined in DNVGL-OTG-13 and as defined by Stansberg (2014).

It is shown in this case study that the maximum free surface elevation calculated with linear diffraction-radiation theory can be severely overestimated over the pontoons in front of upwave columns. We explain the observed discrepancy in this case primarily by a very high linear predicted amplification induced by the shallow pontoon, with resulting high local steepness leading to local breaking and dissipation. Therefore, such pontoon effects should be addressed in semisubmersible platform air-gap analysis. The work also highlights the importance of having good experimental data available when performing such analysis.

INTRODUCTION

The air gap between the top side of an offshore platform and the incoming wave field is an important design parameter that determines if a structure will possibly be subjected to wave slamming loads. In the case of semisubmersible mobile offshore units, calculating air gap is not a trivial task because it requires knowing not only the free surface elevation behavior but also the motions of the floating vessel.

In the early days of offshore oil and gas exploration, air gap analysis on semi-submersibles had to be based on expensive model basin tests. As far as the authors are aware, numerical calculation methodologies started to be proposed and investigated only in the late nineties (Manuel and Winterstein 1999; Sweetman 2001). These methodologies rely mostly on potential flow perturbation theory, solved up to second order, but there are studies where fully nonlinear potential flow methods were used to assess the air gap (Kvaleid, et al. 2014). Since these approaches are not easy to use, research evolved in the sense of providing simplified but accurate approaches for

the assessment of air gap. An example of such research is the work of Sweetman (2004).

Following this trend, DNV (2007) recommended a simplified methodology for calculating air gap, later thoroughly described in the technical note DNVGL-OTG-13 (2017), that has become the industry standard. In this approach, the free surface elevation and the motions of the platform are calculated with linear diffraction-radiation theory, typically combined with a Morison model to include viscous drag loads. The air gap is defined in terms of upwell, or relative motion between the free surface and the deck box, where upwell maxima correspond to air gap minima. Upwell is contributed by wave frequency motions, low frequency motion and mean response, but also by nonlinear free surface elevation. The nonlinear nature of the incoming and diffracted waves is modeled by an amplification factor applied to the free surface elevation response, known as the wave asymmetry factor.

Research on the wave asymmetry factor shows it is influenced not only by nonlinear incoming waves but also by nonlinear diffraction on the floating structure. A good review of the research related to the subject is provided in Stansberg's (2014) work. In that paper, Stansberg suggests an empirical formula for the asymmetry factor that accounts for local steepness of the wave and run-up effects in the region close to the columns. The formula was suggested based upon several sets of model test data, including simple column tests as well as tests with semisubmersibles. Special nonlinear shallow pontoon effects are not included in the formula, but it is noted there that such phenomena should be kept in mind and possibly be taken into account if relevant.

Pessoa and Moe (2016) presented a numerical study of the air gap of a semi-submersible platform with 4 squared columns supported by two longitudinal pontoons. They use the methodology described in DNVGL-OTG-13 and show that the region over the pontoons is the most critical area in terms of upwell. This is mostly due to diffraction effects that cause standing waves in the vicinity on the columns, but is also due to a shallow water effect induced by the top of the pontoons. The former effect increases with the decrease of the depth of water over the pontoons.

The question is if this effect is realistic and if it is corroborated by experimental data. Linear diffraction/radiation theory has been known to overestimate the free surface elevation response in closely bounded regions. A famous example was identified by Buchner et al (2001) on the sloshing of the free surface between two very large vessels floating side by side, in which dissipation induced by flow separation from the ships bilges explained the discrepancy between the numerical and experimental results. The similarity between that problem and the flow over the pontoons, in which water flows over the bilges of the pontoons, is significant.

It is known from the literature that the wave asymmetry factor should be used with care in case the floating platform has shallow draft pontoons. This is suggested by Stansberg (2014) when he applied his version of the wave asymmetry factor to the Veslefrikk B semisubmersible platform. In that case study,

pontoon effects were addressed for positions near aft columns, while at the positions near upwave columns such effects in fact appeared to be small. He further mentions such effect near aft columns had also been observed for another semi platform and suggests that it may be related to wave breaking over the pontoons. In recent research conducted in Wood, similar behavior of the free surface elevation in the region over the pontoons has been observed. Some of these findings were previously shared in the presentation of Pessoa and Moe (2016) work. In the present paper that investigation is documented and further developed.

DESCRIPTION OF THE CASE STUDY

General

The present study deals with the free surface elevation over the pontoons of a semi-submersible platform floating in waves. The free surface response in this location is contributed by incident, diffracted and radiated wave fields. The objective of the study is to assess the limitations of linear radiation and diffraction theory for modelling the flow in this region. For this purpose, the free surface elevation behavior in incoming following seas is analyzed in three different locations under the deck box (see Figure 1):

- Relw 3: located over the pontoon, 1.0m in front of column
- Relw 4: located in the vicinity of the pontoons
- Relw 5: located between the pontoons

Semisubmersible Platform Data

The semi-submersible used in the present case study has four rectangular columns supported by two longitudinal pontoons. The columns on each side of the vessel are connected by four horizontal bracings. The vessel is moored with a soft mooring system.

The study is performed in two draughts, representing operating and survival modes. The characteristics of the semi-submersible platform in the two draughts are presented in Table 1.

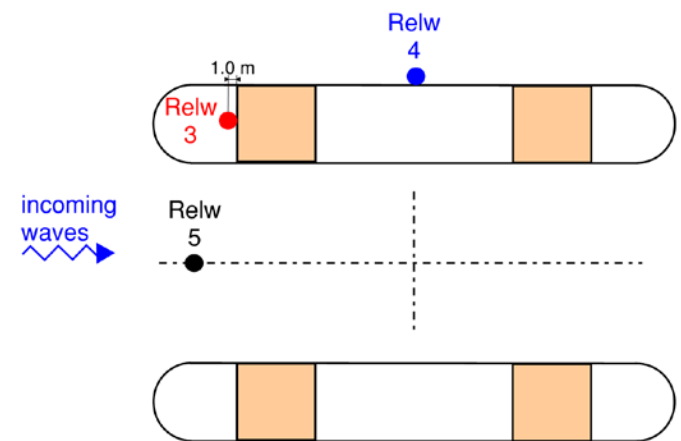


Figure 1 Locations where free surface elevation is assessed

Model tests

Model tests have been performed at a model scale of 1:38.89. The model was held in place by a linear 4 line horizontal mooring system, symmetrical with respect to centerline and to mid ship.

Upwell was measured by relative wave gauges fixed to the vessel at the locations shown in Figure 1. The free surface elevation is obtained by removing the combined vertical motion from the upwell signal, using the global motions of the vessel to derive the combined vertical motion in each location. This procedure is performed in the time domain. Incoming wave elevation was measured at the center of the reference system during calibration runs without the model in place.

The analyzed conditions, which include both regular waves (characterized by wave period T and wave height H) and irregular waves (characterized by peak period T_p , significant wave height H_s and peak enhancement factor γ), are summarized below:

- Jonswap spectrum, $H_s = 2.0$ m, $T_p = 8.3$ s, $\gamma = 3.3$
- Jonswap spectrum, $H_s = 4.5$ m, $T_p = 9.6$ s, $\gamma = 3.3$
- Jonswap spectrum, $H_s = 7.0$ m, $T_p = 11.0$ s, $\gamma = 3.3$
- White noise spectrum, $H_s = 3.5$ m
- Regular waves, $H = 3.5$ m with $T = 6$ s, $T = 8$ s, $T = 9$ s, $T = 10$ s, $T = 12$ s and $T = 14$ s

Each condition was measured in a single run, with 10000 s duration in irregular seas and 375 s in regular waves.

Numerical model

The flow is calculated with linear diffraction and radiation theory, using a 3D boundary element method (also known as panel method) to enforce the linearized boundary conditions and calculate a velocity potential. A lower order panel mesh with 2682 panels for half of the wetted surface in operation draught (shown in Figure 2) and 2272 panels in survival draught was used on the calculations. Convergence of the numerical free surface elevation results with respect panel mesh has been confirmed.

A Morison model of the horizontal bracings, pontoons and columns is included to calculate drag forces and viscous damping of the wave-frequency motions. The Morison elements are scaled so that only drag loads are included in the numerical model. Drag coefficients are calibrated based on comparisons with experimental results. Drag forces are linearized with a stochastic approach in each of the tested conditions.

It is reasonable to consider that the soft mooring system does not influence the wave frequency motions of the vessel. It was therefore assumed that the vessel is freely floating.

Numerical free surface response amplitude operators

Given the described test case and numerical model, the free surface elevation response amplitude operators (RAOs) shown in Figure 3 are found. The plots include the response in survival and operation draughts in the three locations defined for the study. Free surface RAO in the location over the pontoons (Relw 3) is represented by a solid red line.

Table 1 characteristics of the semi-submersible platform

		operation	survival
Width of pontoons	m	16.50	16.50
Depth of pontoon top	m	7.45	5.45
Width of squared columns	m	15.50	15.50

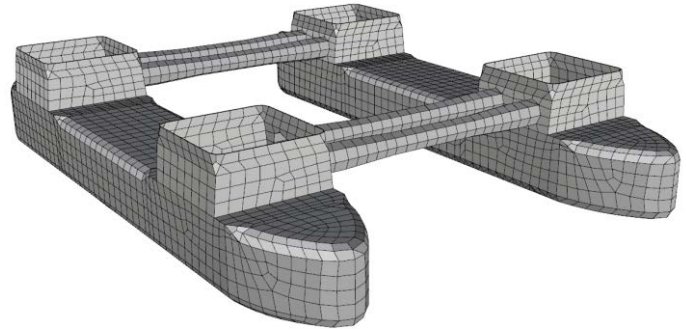


Figure 2 Panel mesh distribution in operation draught

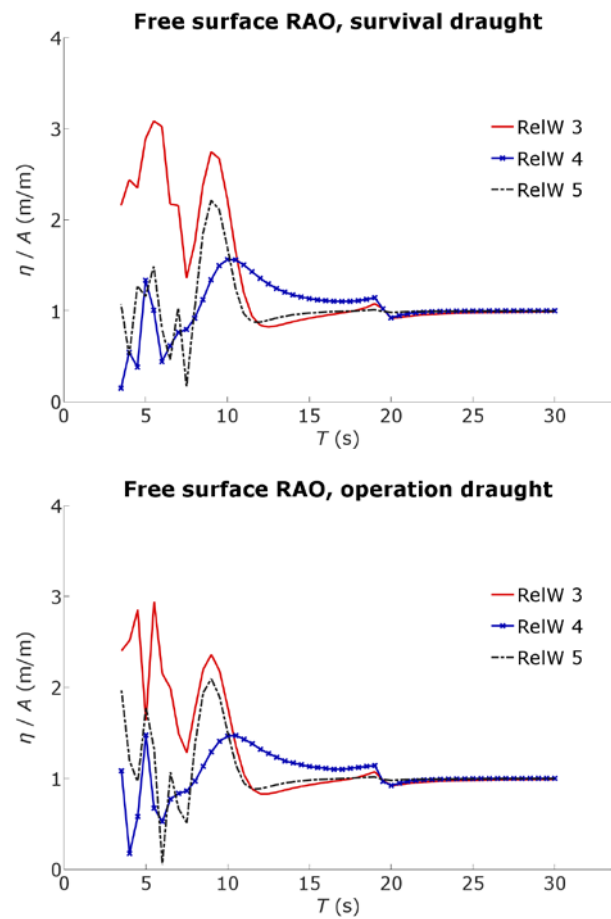


Figure 3 Free surface elevation (η) RAOs (A is the incident wave amplitude) in the three locations in survival (top plot) and operation (bottom plot) draughts

The results show that flow in the short period range (3 s – 15 s) is strongly affected by the diffracted wave field. This is evidenced by the significant peaky behavior of the curves in this range. In the long period range (15 s – 30 s) the curves are close to unity, meaning that the flow is dominated by the incident wave field and is hardly affected by the presence of the structure. This means that amplification of the free surface will not likely occur in long periods, but it may be significant in short periods. In addition, semi-submersible vessels have typically very low vertical response in the short period range, thus contributing to increase upwell. As a result, air gap reduction may be more critical in sea states with short T_p and low H_s than in sea states with long T_p and high H_s . In our experience, this is commonly the case.

It is clear that the free surface response over the upwave pontoons (Relw 3) is significantly amplified in the short period range. The linear amplification factor (seen from the RAOs) is between 2.5 and 3 around wave periods 9 s and 6 s, which is significantly high, while it reaches a maximum of about 2 at the other locations. This is in part due to shallow water shoaling effect – note that the response in operation draught, which has higher pontoon submergence, is slightly lower – but also due to very strong focusing of waves in front of the columns. The actual widths and geometries of the columns and pontoons may also play a role here. The implication of this phenomenon in terms of air gap is significant and is the motivation for the present case study.

NUMERICAL RESULTS AND COMPARISON TO MODEL TEST DATA

Irregular waves: motion and upwell response spectra

As described in the previous section, upwell is measured by relative wave gauges fixed to the floating vessel. The free surface elevation is then calculated by removing the vertical motion from the upwell signal. Considering the radiated wave field, good agreement of free surface computations with the experiments is also dependent on the dynamics of the vessel in waves being well reproduced by the numerical model. Such agreement is evidenced in Figure 4, where wave, heave, pitch and upwell auto spectra in a sea state with $H_s = 4.5$ m and $T_p = 9.6$ s are presented, and in Figure 5 where equivalent results are shown for a sea state with $H_s = 7$ m and $T_p = 11$ s. The plots show both experimental results and numerical computations. The following key observations can be made from the presented results:

- The incident wave spectra are well represented by its numerical models. Energy of the sea state is significant in periods ranging 4 s – 15 s in Figure 4 and ranging 5 s – 17 s in Figure 5.
- The heave and pitch numerical response is in very good agreement with the experiments in the medium period range (7 s – 15 s). The response in the short period range (4 s – 7 s) is negligible.

- Numerical upwell response is in good agreement with the experiments in the three tested locations in the short to medium period range (4 s – 13 s), albeit slightly overestimating the peak energy in Relw 3 and Relw 4 locations, in the least energetic sea state. In the more energetic sea state, the discrepancy in Relw 3 peak energy is more significant.
- There is significant response in heave and pitch on the long period range (> 15 s) which is not captured by the linear numerical model. This is most likely caused by second order low frequency wave loads inducing resonant motions. These are not accounted for in linear numerical models. Upwell response in the long period range (> 15 s) in these sea states is however almost negligible and wave radiation is likely non-existent. The low frequency discrepancy is thus not relevant for modelling the wave frequency free surface elevation.
- Upwell response in the location over the pontoons (Relw 3) is significantly higher than the other locations, which is consistent with what is observed in Figure 3.

Given the above considerations, it can be concluded that the numerical model is able to correctly capture the motion dynamics of the system in the most relevant period range (3 s – 15 s), and is thus appropriately calibrated to be used in the present investigation.

Irregular waves: free surface elevation response statistics

The free surface elevation dynamics in irregular wave is studied in terms of linear and higher order statistics, which are presented in Figure 6. The presented statistics include standard deviation, skewness, excess of kurtosis and maximum crests in all three locations and in both of the tested draughts. Numerical computations have been performed for the standard deviation and for the maximum crests, using standard spectral theory. The maximum surface crests results are compared with nonlinear numerical estimations computed with two different approaches for calculating the wave asymmetry factor. The first approach is Stansberg's (2014) empirical prediction procedure, where the diffracted wave amplitude is dependent on the local wave steepness parameter kA and the distance to the columns. In the formula, the free surface is affected by the wall effect only if it is located less than a column width away from the column, but it always affected by the local steepness parameter. The second approach is the wave asymmetry factor recommended in DNVGL-OTG-13 (March 2017). In this approach the wave asymmetry is defined in general as equal to 1.2. In some special circumstances, wave asymmetry should be taken as 1.3 - that is the case in the Relw 5 location. In regions close to the column – which is the case in Relw 3 location – DNVGL-OTG-13 (March 2017) refers to Stansberg (2014) formula. We use in this case a factor of 1.3. Finally, the plots show also the free surface crest if Gaussian behavior is assumed, given by the most likely maximum considering the same sea state characteristics and duration.

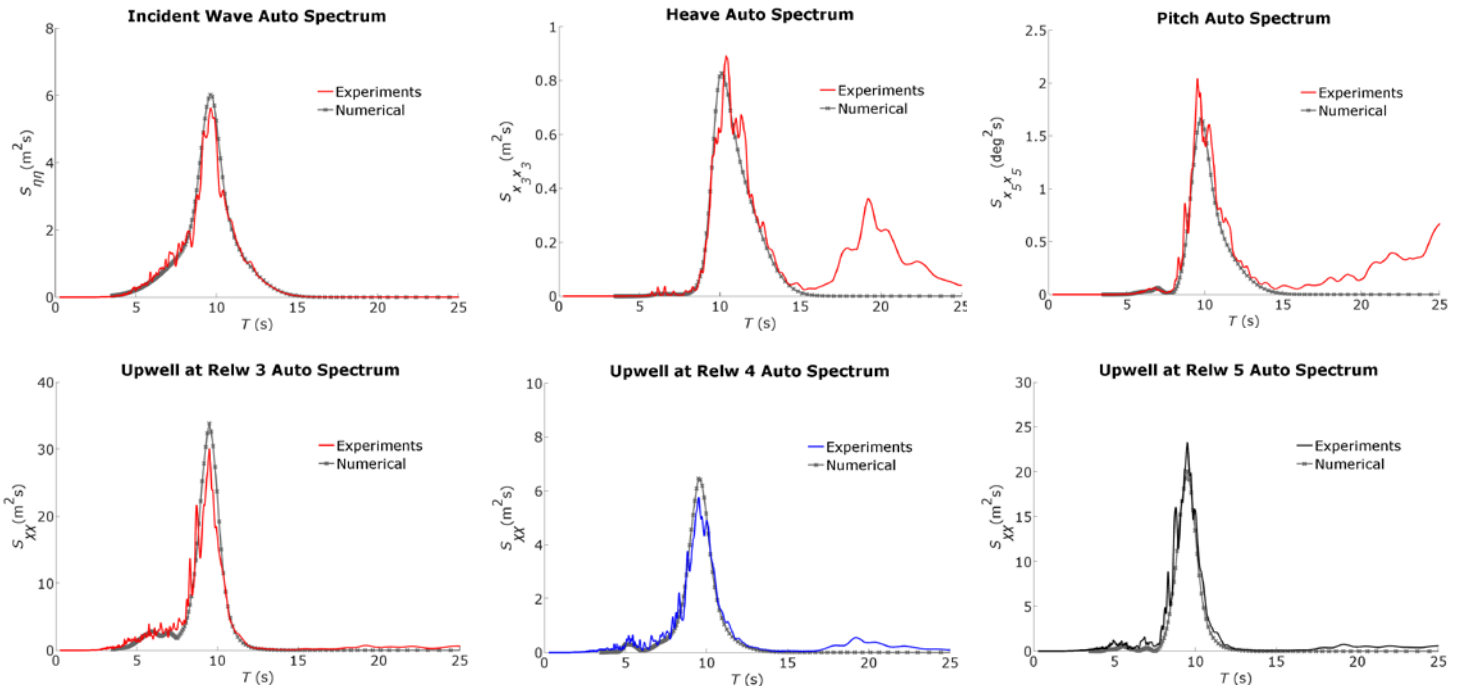


Figure 4 Incident wave, heave, roll and upwell auto spectra in survival draught, in a sea state with $H_s=4.5m$ and $T_p=9.6s$

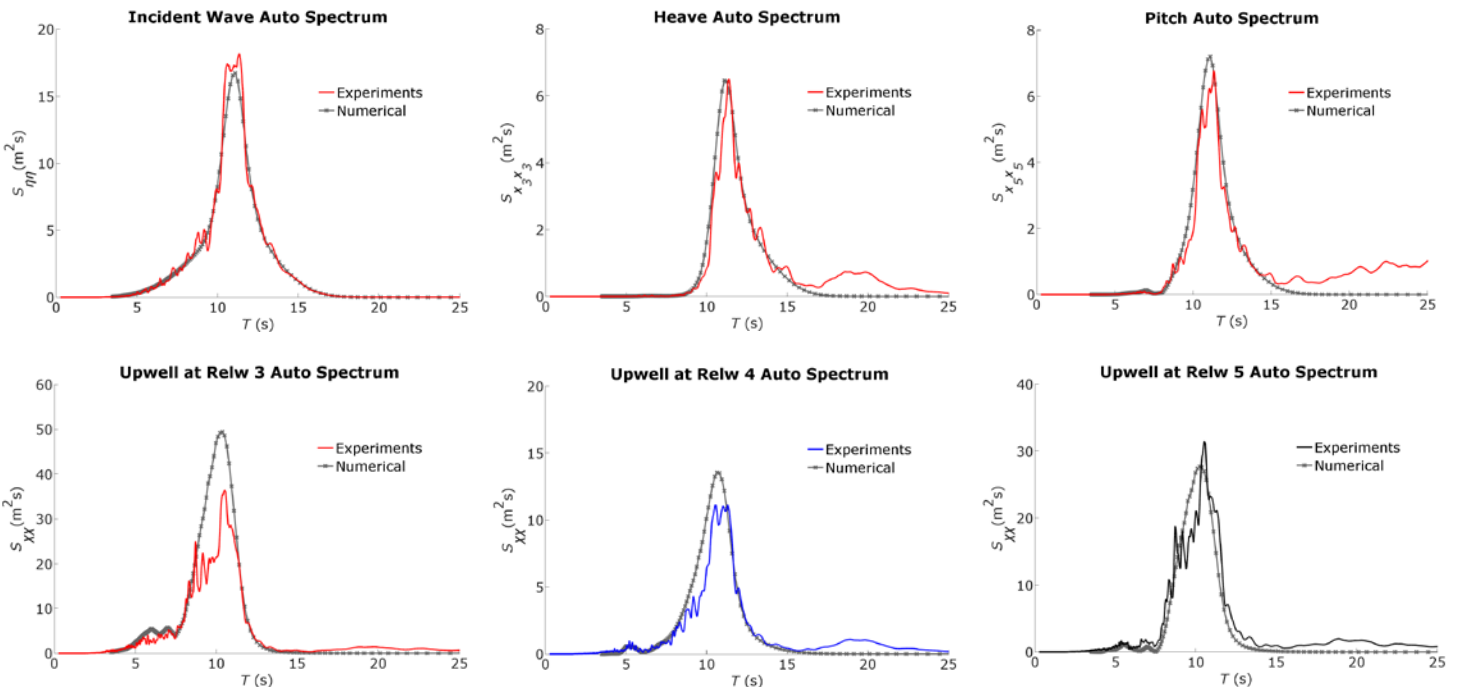


Figure 5 Incident wave, heave, roll and upwell auto spectra in survival draught, in a sea state with $H_s=7.0m$ and $T_p=11.0s$

The following key observations are made:

- The measured standard deviations are fairly similar to the numerical ones, except from a numerical over prediction for Relw 3 in the two largest sea states, and a slight under prediction for Relw 5 in the two lowest sea states. This can

also be seen from the corresponding power spectra. The under prediction for Relw 3 is most likely due to dissipation and breaking, as a result of a very strong amplification around $T = 6 s$ and $T = 9 s$ as seen in Figure 3, combined with local shallow pontoon effects (local refraction).

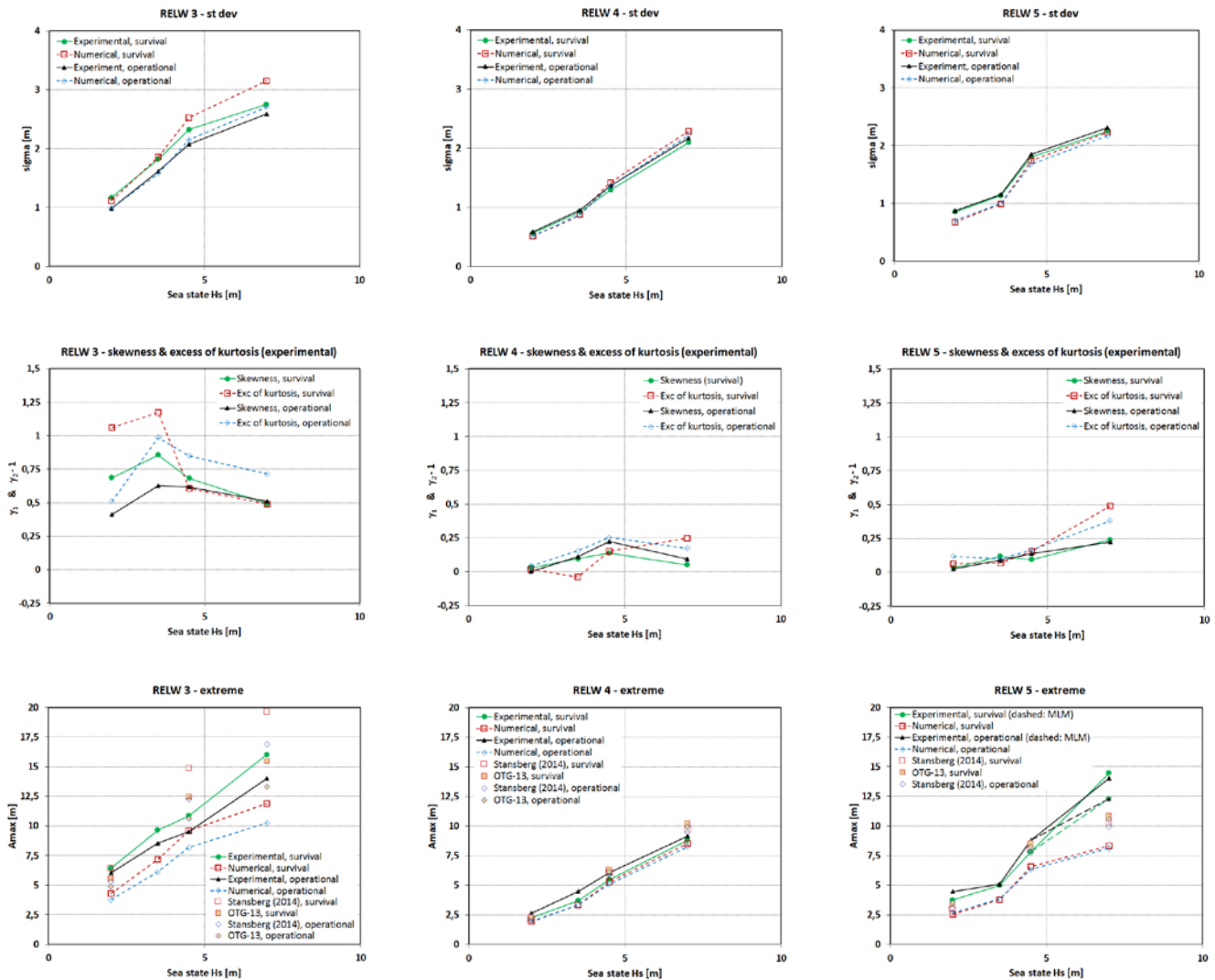


Figure 6 Standard deviation (top), skewness and excess of kurtosis (mid), and extreme value (bottom) of free surface elevation in the three studied locations, found in simulations with the linear model and experiments in irregular sea states, plotted as function of significant wave height

- The overestimation of the standard deviation in Relw 3 location is more significant in survival draught than in operation draught, indicating a relation with the shallow water effect induced by the pontoons.
- The pontoon effects for Relw 3 can also be recognized from the skewness and kurtosis plots: Very high skewness and kurtosis values are observed especially for the two lowest sea states, due to nonlinearities as a result of the strong amplification in the RAO and the shallow pontoon. The kurtosis and skewness values in Relw 3 are somewhat reduced (but still high) for the highest sea states, which can be explained by a local breaking and dissipation process - we have observed similar effects in shallow and finite water breaking waves. For Relw 4 and Relw 5, the skewness and kurtosis values are more moderate and similar to those for undisturbed waves. The relatively high kurtosis for Relw 5

in $H_s = 7$ m is probably a random sampling variation effect which can be related to a particularly high random event (see below).

- For the extreme crests, we again see particular effects for Relw 3, where the predicted values from Stansberg (2014) and OTG-13 are clearly over predicting the observed values; this can be related to the local breaking and dissipation mentioned above. Similar effects had been observed in the experimental data sets used in Stansberg (2014), but for aft columns only, not upwave. Physically one can explain the present observation by two related effects: Energy dissipation (a reduction in standard deviations, see above), and less non-Gaussian behavior for the largest peaks after the breaking. For Relw 4 the crests are similar to the two nonlinear models, and only slightly higher than the linear predictions. For Relw 5 in the highest

sea state ($H_s = 7$ m), the measured extremes are clearly higher than the predicted ones; however in this case this is due to a random single event much higher than the others; the most likely highest peak from a Weibull fitting are lower as indicated on the plot.

- Nonlinear effects in Relw 3 are expected to be contributed by wave asymmetry, shallow water shoaling due to the presence of the pontoons and run-up effects due to the presence of the column, all contributing in the sense of enhancing free surface crest. In the Relw 5 location, nonlinearity is more likely related to just wave asymmetry. These assumptions are confirmed by the higher order statistical parameters. It would therefore be expected a larger nonlinear amplification of the extremes in Relw 3 than in the extremes in Relw 5. That is clearly not the case, and that can be justified by the dissipation effect in Relw 3 described above.

It should be mentioned that, on the sea state with $H_s = 7$ m, the measured peaks in Relw 3 location have a source of uncertainty due to instrumentation challenges. We believe that the accuracy in that case is within 0.5m - 1m. Furthermore, an apparent truncation of the troughs is present in the time series. This is caused by the presence of the pontoon and it contributes to a slight reduction of the standard deviation. We estimate this reduction to be in the order of 3%-4%. This is also influencing the skewness and kurtosis, compared to a model without such truncation, as is the case of the numerical computations. In future work we may simulate truncated numerical signals according to the observed phenomena in order to have more consistent comparisons.

Regular waves: first harmonic of the free surface elevation response

Free surface elevation response amplitude operators are presented in Figure 7 for the tested locations and draughts. The plots show a comparison of the numerical results with the first harmonic of the experimental response, which is obtained by filtering of the experimental signal (an example of this filtering process is shown in Figure 9). The goal is to remove the asymmetry effects induced by the over harmonics in order to have a completely linear response in the comparison. It was not possible to achieve the exact input wave periods at the basin, as shown in Table 2. Experimental results are therefore plotted as function of the achieved periods. It should be mentioned that results for $T = 6$ s are somewhat uncertain due to unstable wave trains arising from nonlinear instability modulations.

The measured local steepness parameter (given as kA_0 , where k is the wave number of the measured response and A_0 is the 1st harmonic amplitude of the disturbed free surface elevation) for this set of data is presented in Table 3 for survival draught and in Table 4 for operation draught.

The results show in general very good agreement between experiments and numerical computations in the Relw 4 and Relw 5 locations, although there is a slight overestimation of the results in the Relw 4 in survival draught in $T = 10$ s and $T = 12$ s. The numerical computations in the location over the

pontoons (Relw 3) significantly overestimate the experimental data in both survival and operation draughts, albeit more expressively in survival draught. This is consistent with what is observed in irregular waves. The reason for the discrepancy is not completely clear. One could expect some possible wave breaking and dissipation in $T = 6$ s, where the local steepness is very high, but that is the period where the best agreement is observed. In addition, the local steepness in Relw 5 location is comparable to the local steepness in Relw 3 location; nonetheless the agreement in Relw 5 is very good. This shows that the higher steepness of the response in Relw 3 is not responsible for the observed discrepancy.

Nevertheless, the experimental results over the pontoons confirm qualitatively some of the observed phenomena in the numerical computations:

- Strong amplification of the free surface elevation over the pontoons in $T = 6$ s and $T = 9$ s, confirming the diffraction effects in the short period range.
- Larger amplification over the pontoons in survival draught than in operation draught, confirming the shallow water shoaling effect.

Regular waves: Free surface elevation crests

The measured free surface elevation crests in regular waves are presented in Figure 8 normalized by the incident wave amplitude. The results are compared with non-linear numerical estimations computed with two different approaches for calculating the wave asymmetry factor, namely as defined in Stansberg's (2014) and as defined in DNVGL-OTG-13. The approaches are primarily intended for use in irregular sea states, but it is also of interest here to see how well they perform for regular waves. According to recommendations given in DNVGL-OTG-13, the asymmetry factor is chosen as 1.2 in Relw 4 and as 1.3 in Relw 5 locations. There was a draft version of the DNVGL-OTG-13 (September 2016) in which a variation of Stansberg's formula was presented, where the local steepness dependence was substituted by a 1.2 factor. While DNVGL is no longer suggesting that formula, it is still interesting to evaluate its accuracy. For this reason, the formula is used in the computations for Relw 3 location. The plots show also the free surface crest if linear behavior is assumed.

Table 2 Input wave period vs achieved wave period (s)

Input	6.00	8.00	9.00	10.00	12.00	14.00
Achieved	6.01	7.91	8.84	10.02	11.56	13.66

Table 3 Local steepness kA_0 in survival draught

T (s)	6.01	7.91	8.84	10.02	11.56	13.66
Relw 3	0.439	0.122	0.173	0.099	0.014	0.021
Relw 4	0.056	0.099	0.094	0.089	0.065	0.042
Relw 5	0.164	0.118	0.169	0.112	0.038	0.033

Table 4 Local steepness kA_0 in operation draught

T (s)	6.01	7.91	8.84	10.02	11.56
Relw 3	0.395	0.122	0.147	0.101	0.033
Relw 4	0.091	0.104	0.098	0.095	0.067
Relw 5	0.076	0.133	0.173	0.107	0.040

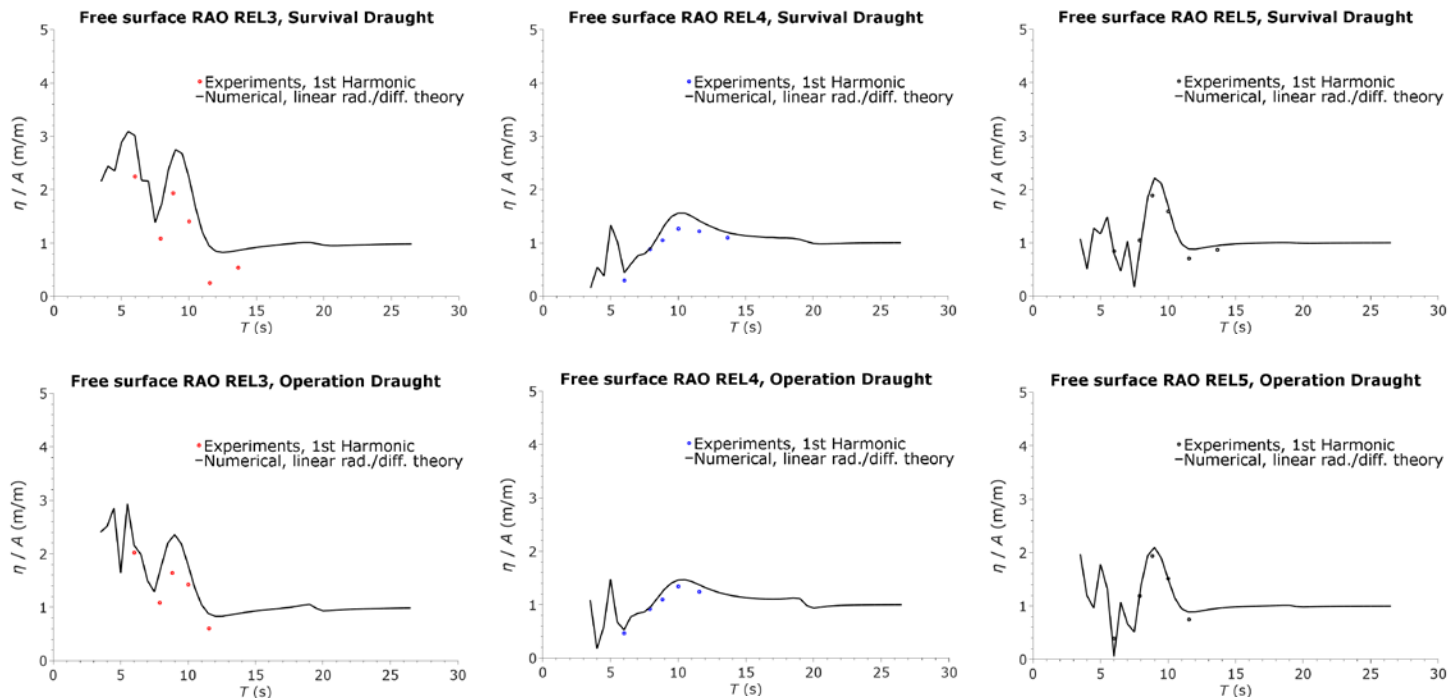


Figure 7 Free surface elevation response amplitude operators in the three studied locations. First harmonic of the experimental signal vs numerical computations with linear diffraction and radiation theory.

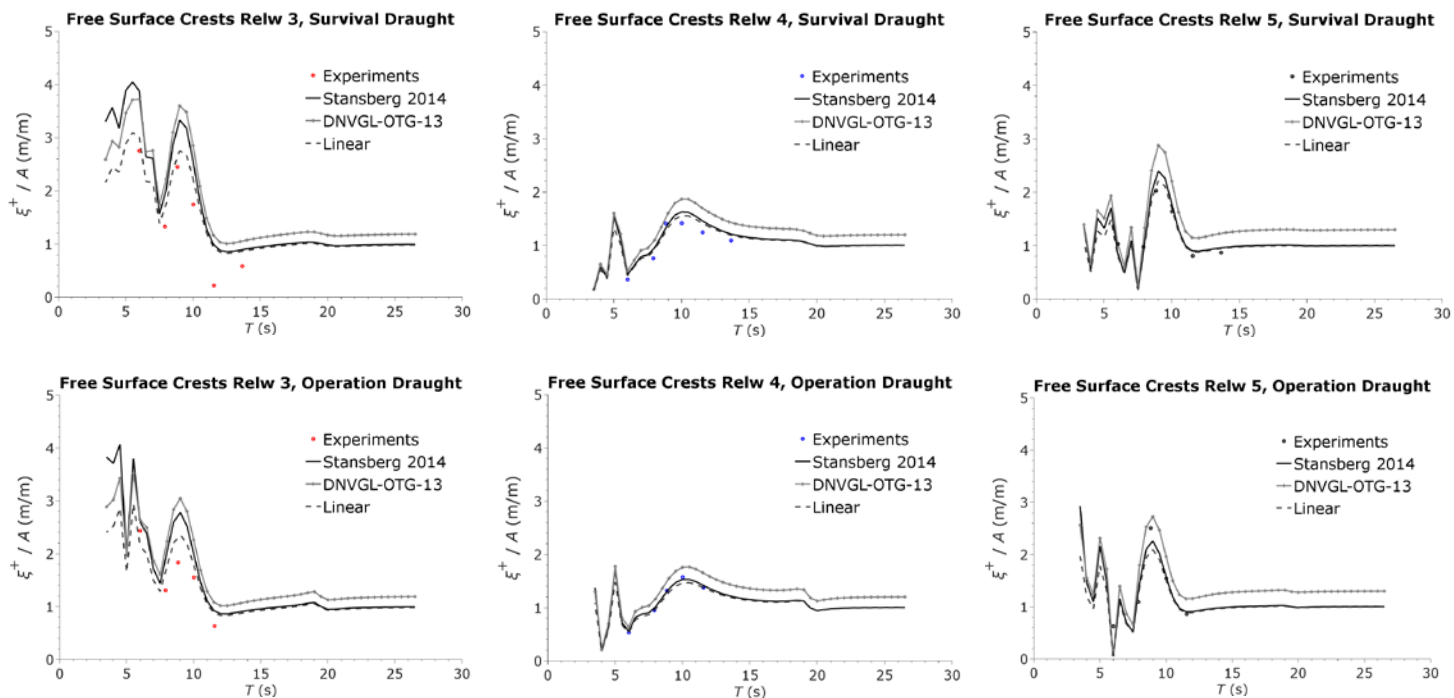


Figure 8 Free surface crests (ξ^+) normalized by the incident wave amplitude (A) in the three studied locations. Experimental and numerical computations with linear and nonlinear methods

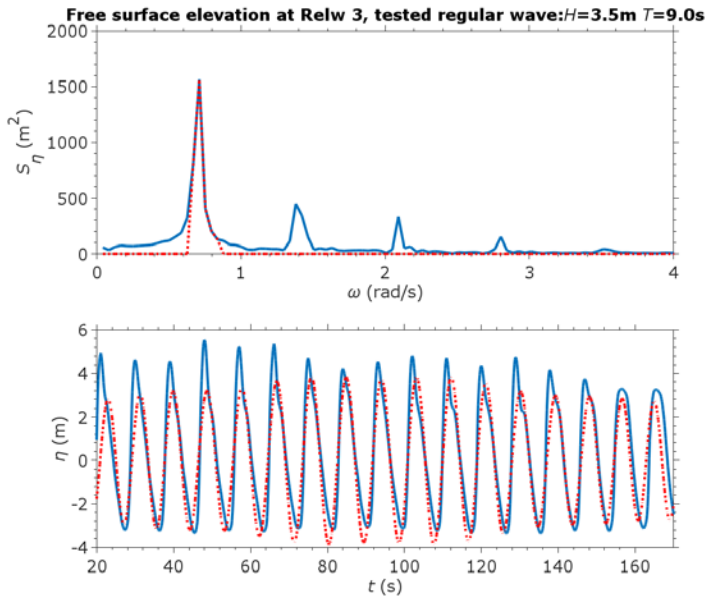


Figure 9 Free surface elevation response spectrum to an incident regular wave with $T = 9.0$ s and $H = 3.5$ m. Filtered first harmonic (dotted red) and original (solid blue) signals

The following key observations are registered:

- DNVGL-OTG-13 formula is conservative, as it tends to overestimate the experimental data in all of the tested conditions.
- Local steepness in Relw 5 is generally low (see Table 3 and Table 4) and the location is outside the region influenced by the wall. As a consequence, Stansberg (2014) formula is almost linear. The experimental results seem to confirm this, as the agreement of this numerical model with the experiments is very good in both of the tested draughts.
- Results in the vicinity of the pontoons (Relw 4) are slightly overestimated by Stansberg formula in survival draught, but in very good agreement in operation draught.
- Since the results in Relw 4 and Relw 5 are approximately Gaussian, DNVGL-OTG-13 formula overestimates the observed crests in these locations in about 20 % to 30 %.
- The results in Relw 3 location are significantly overestimated by the nonlinear models. This effect is more expressive in survival draught than in operation draught.
- The results in Relw 3 location are in better agreement with the linear model than with the nonlinear models. This is unexpected since the response in this location is significantly nonlinear, as evidenced by the kurtosis and skewness parameters shown in Figure 6. The reason for apparent better agreement is likely to be a bias related to the observed discrepancy in the results shown in Figure 7.
- The previous comment is also supported by Figure 9, showing the response spectrum of the free surface elevation in Relw 3 location, in the $T = 9.0$ s run. There is significant energy present in the over-harmonics which is a clear deviation from the linear assumption.

CONCLUSIONS

The paper presents an investigation on the free surface elevation over the pontoons of a semi-submersible platform in waves. Numerical computations with linear diffraction theory have been compared to experimental measurements acquired over the pontoons. The free surface elevation was also measured in two other locations.

The numerical computations show significantly high amplification of the free surface elevation over the pontoons near upwave columns. This is induced by a shallow water shoaling effect and by wave focusing in front of the columns. This was qualitatively confirmed by the experimental data.

The flow over the pontoons exhibits highly nonlinear and non-Gaussian behavior, which is evidenced by higher order statistics parameters skewness and kurtosis. The nonlinearity is increased with the decrease of the submergence of the pontoon top. This induces significant nonlinear enhancement of the free surface crests.

The correlation of the experimental measurements of the free surface over the upwave pontoons to the numerical computations is, however, not perfect. The numerical calculations significantly overestimate the measured response in all of the tested conditions. The correlation in the other locations was very good, indicating that the discrepancy is particular to the flow over the pontoons. The discrepancy is increased with the decrease of the submergence of the pontoon top, which indicates that it may be related to the shallow water effects.

The mechanism for energy dissipation is not yet fully understood. However we believe that it is likely related to the very high numerically predicted RAO peaks observed above the upwave pontoon in this case for waves with T shorter than 11s, which may predict unphysical amplification leading to locally very steep peaks and thereby local wave breaking. Another possible source for dissipation may be related to the water flowing over the bilges of the pontoons, which may lead to flow separation that is not accounted for by the numerical model. This subject deserves more investigation. In conclusion, we recommend that possible nonlinear shallow pontoon effects should be addressed to assess when it is relevant and, if needed, taken it into account. The work also highlights the importance of good model test data in such analysis.

ACKNOWLEDGMENTS

The present work is presented with kind permission from Wood Norway. The authors also appreciate the role played by FORCE Technology.

REFERENCES

- DNV-RP-C205, *Environmental Conditions and Environmental Loads*. April 2007. DNV.
- DNVGL-OTG-13, *Prediction of air gap for Column Stabilised Units - Draft*. September 2016. DNVGL.
- DNVGL-OTG-13, *Prediction of air gap for Column Stabilised Units*. March 2017. DNVGL.
- Buchner, B., Dijk, A. and Wilde, J., 2001, Numerical multiple-body simulation of side-by-side mooring to an FPSO, *Proceedings of*

- the Eleventh International Offshore and Polar Engineering Conference, Stavanger, Norway, Vol. I, pp343-353.
- Kvaleid, J., Oosterlaak, V., and Kvillum, T., Nonlinear Air Gap Analysis of a Semisubmersible Compared With Linear Analyses and Model Tests, *Proc.*, ASME 33rd International Conference on Ocean, Offshore and Arctic Engineering, San Francisco, California, June 8-13, OMAE2014-24044.
- Manuel, L. and Winterstein, S.R., 1999, Air gap response of floating structures under random waves: analytical predictions based on linear and nonlinear diffraction, oral presentation at the 18th International Conference on Offshore Mechanics and Arctic Engineering, St. John's, Newfoundland, Canada, July 11-16, Paper No: 99-6041.
- Pessoa, J. Moe, A., Air Gap on Semisubmersible MODUs Under DNVGL Class - Current & Future Design Practice – (referred results were shown only on the presentation slides), Offshore Technology Conference (OTC2017), 1-4 May, Houston, Texas, OTC-27693-MS.
- Stansberg, C., 2014, Nonlinear wave amplification around column-based platforms in steep waves. *Proc.*, ASME 33rd International Conference on Ocean, Offshore and Arctic Engineering, San Francisco, California, June 8-13, OMAE2014-24569.
- Sweetman, S., 2001, *Air Gap Analysis of Floating Structures Subject to Random Seas: Prediction of Extremes Using Diffraction Analysis Versus Model Test Results*. PhD thesis, Stanford University, Stanford, California (August 2001).